12th International Symposium on Turbulence and Shear Flow Phenomena (TSFP12)
Osaka, Japan (Online), July 19-22, 2022

INTERPRETATION AND PREDICTION FOR PRANDTL NUMBER EFFECT IN TURBULENT HEAT TRANSFER USING GENERATIVE ADVERSARIAL NETWORKS

Hyojin Kim
Department of Mechanical Engineering
Yonsei University
50 Yonsei-ro, Seodaemun-gu, Seoul 03722
gywls072@yonsei.ac.kr

Junhyuk Kim
Department of Mechanical Engineering
Yonsei University
50 Yonsei-ro, Seodaemun-gu, Seoul 03722
junhyuk6@yonsei.ac.kr

Changhoon Lee
School of Mathematics and Computing
Yonsei University
50 Yonsei-ro, Seodaemun-gu, Seoul 03722
clee@yonsei.ac.kr

ABSTRACT

We propose a interpretable deep learning model that embedded effect of physical parameter in turbulence. Turbulence is a very complex flow, and the analysis of relationships between turbulent variables remains a fundamental challenge. Recently, studies applying deep learning are being conducted in attempts to analyze turbulence. Deep learning can extract physics features in data, which is turbulent analysis model to understand the physical relationship between variables in turbulent flows. In this study, we consider turbulent heat transfer to extract and analyze the effect of Prandtl number (Pr) in the data. The deep learning model uses conditional generative adversarial networks (cGAN) with decomposition algorithm. Our model predicts surface heat flux with various Pr from wall shear stresses in channel flow. The predicted surface heat flux reflected the characteristics with respect to Pr well, and also was statistically very similar to DNS. We analyzed the spatial nonlinear relationship between wall shear stresses and surface heat flux for Pr through gradient maps of trained our model. Furthermore, for analysis of effect of Prandtl number, we observed decomposed field into universal and Pr-dependent features based on turbulent data sets. Through interpretation of the deep learning model, it is possible to understand the physical interaction between variables, which can help to develop a turbulence model considering physics.

INTRODUCTION

Turbulent heat transfer is an important phenomena observed in science and engineering fields, and there are the examples such as gas turbines, heat exchangers and nuclear reactors. The close analogy between temperature fluctuations and momentum is well known, resulting in a high similarity between heat flux and shear stress at the wall (Antonia *et al.*, 1988; Kim & Moin, 1989; Kasagi *et al.*, 1992). However, the distribution of heat flux is highly depending on Prandtl number ($Pr = \nu/\alpha$; ν and α are kinematic viscosity and thermal diffusivity, respectively.), and the strong nonlinearity between the shear stress and heat flux is observed. Many studies using direct numerical simulation (DNS) have been conducted to investigate the effect of Prandtl number (Kasagi & Ohtsubo, 1993; Kawamura *et al.*, 1998), but the observation of local heat flux with Pr has not been sufficiently performed because it is mostly limited to the conventional statistical approach. In fact, the turbulent transport mechanism of heat and momentum near the wall occurs very locally and intermittently due to the role of streamwise vortical structures. The dissimilarity between heat flux and streamwise shear stress is obviously found in some regions, although there is a high correlation between them (Abe *et al.*, 2004).

In this study, we focus on the revealing the complicate relation between the local heat flux and wall-shear stresses with the Prandtl number-effect through deep learning (DL). Unlike the traditional approach, DL can find a nonlinear mapping function between variables and predicts instantaneous fields with high accuracy, showing excellent performance in many turbulence problems (Kim & Lee, 2020; Kim *et al.*, 2021; Güemes *et al.*, 2019, 2021). Although DL performed well in discovering interrelationship between input and output in various turbulence problems, but there are still unresolved fundamental questions about how DL learns turbulence, what characteristics of turbulence DL learns, and which information is essential for prediction. To take a step forward, understanding and interpretation of DL is research of substance. Recently, there are a few attempts to interpret DL with embedded features of turbulence (Kim & Lee, 2019; Lu *et al.*, 2020; Jagodinski *et al.*, 2020), but it is still difficult to provide sufficient answers to these fundamental questions. Therefore, we apply deep learning to predict the surface heat flux with various Pr from wall shear stress, and further investigate the physical phenomena between local heat flux and shear stress through the interpretation of the trained model with the embedded of the Prandtl number effect. The interpretable DL model could help to provide an framework in which discover unknown physical phenomena in the data. In addition, interpretation of DL would play a very important role in the development and per-

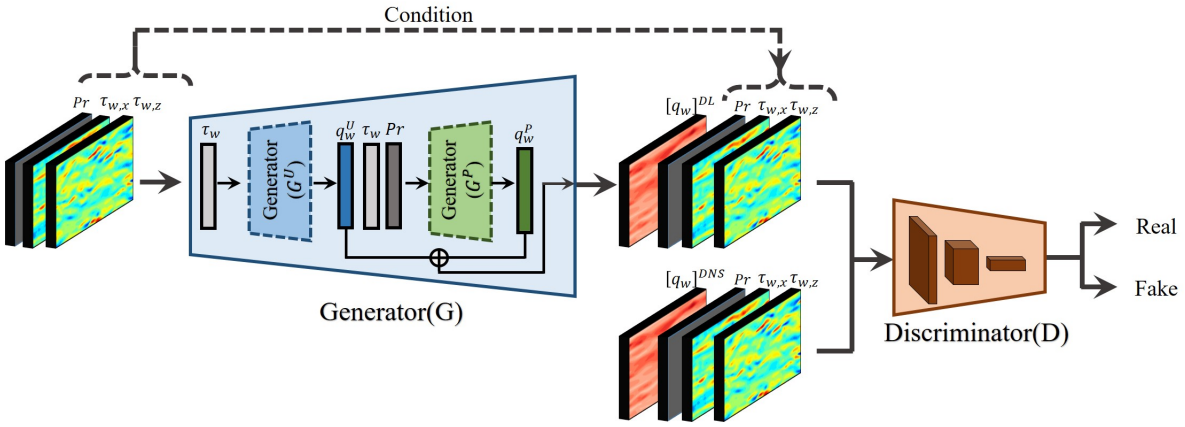

Figure 1. Architecture of conditional generative adversarial networks (cGAN) with decomposition algorithm.

formance improvement of itself and for providing the guidance of DL construction (e.g., hyper parameter optimization).

METHODOLOGY

Data collection

To collect datasets for training of the DL model, we performed DNS of turbulent channel flow with passive temperature. The mean flow in streamwise direction is driven by a constant pressure gradient. The constant temperature and no-slip conditions are imposed at both walls, and periodic boundary conditions are used in the horizontal directions. The governing equations are the continuity equation, the incompressible Navier–Stokes equation and the energy equation, as follows:

$$\frac{\partial u_i}{\partial x_i} = 0, \tag{1}$$

$$\frac{\partial u_i}{\partial t} + u_j \frac{\partial u_i}{\partial x_j} = -\frac{\partial p}{\partial x_i} + \frac{1}{Re_\tau} \frac{\partial^2 u_i}{\partial x_j \partial x_j}, \tag{2}$$

$$\frac{\partial T}{\partial t} + u_j \frac{\partial T}{\partial x_j} = \frac{1}{PrRe_\tau} \frac{\partial^2 T}{\partial x_j \partial x_j}, \tag{3}$$

The equations are nondimensionalized by channel half width δ, friction velocity u_τ and temperature difference ΔT between top and bottom walls. $x_1(x)$, $x_2(y)$ and $x_3(z)$ denote streamwise, wall-normal and spanwise direction, respectively. The corresponding velocity components are $u_1(u)$, $u_2(v)$ and $u_3(w)$, respectively. The dimensionless parameters are friction Reynolds number($Re_\tau = u_\tau \delta / \nu$), which is fixed at 180 and molecular Prandtl number, ranging from 0.1 to 7.

Spatial discretization in the horizontal direction and the wall-normal direction used a pseudo-spectral method using Fourier expansion and a central difference scheme, respectively. The second-order Adams–Bashforth and Crank–Nicolson schemes were applied for the temporal integration of the nonlinear and viscous terms, respectively. The domain size is $4\pi\delta \times 2\delta \times 2\pi\delta$ for all Pr, and the number of grid points for $Pr = 0.1 - 1$ and $Pr = 2 - 7$ is $128 \times 129 \times 128$ and $192 \times 129 \times 192$, respectively.

The collected data are wall-shear stresses and surface heat flux of various Pr, and are divided into training, validation, and testing data. The testing data are sufficiently decorrelated from the training data.

Deep learning model

Conditional generative adversarial network (cGAN) is used for prediction and interpretation of surface heat flux with various Pr. In figure 1, cGAN consists of two networks, generator (G) and discriminator (D), and is trained through competitive learning of these two networks. The input data is used for the discriminator as conditioning, and this constraint allows the generator to generate output image dependent on the input one. Finally, we can obtain a generator that generates a fake image similar to the real image while being dependent on the input data. This process can be described as a min/max problem, and the loss function used for training is as follows:

$$\min_G \max_D \mathbb{E}_{y\sim P_Y}[\log D(y|x)] + \mathbb{E}_{x\sim P_X}[\log(1 - D(G(x)|x))], \tag{4}$$

In this study, x is the streamwise and spanwise wall shear stress and Prandtl number, and y is the surface heat flux for Pr. Additionally, for in detail analysis of the Pr-effect, we applied a decomposition algorithm to cGAN that can separate surface heat flux into universal features q_w^U and Pr-dependent features q_w^P. For the extraction of the Pr-effect, the generator is divided into a universal generator G^U and the parameter effect generator G^P. G^U generates universal features that have common characteristics of surface heat flux for all Pr from wall shear stresses. G^P extracts Pr dependent features with properties for the Pr-effect from the wall shear stress and Prandtl number. Finally, the surface heat flux ($q_w = q_w^U + q_w^P$) can be obtained as the sum of the decomposed features, and the total loss function for training of the model is as follows.

$$\mathscr{L}_{total} = \mathscr{L}_{cGAN} + \lambda_1 \mathscr{L}_{mse} + \lambda_2 \mathscr{L}_{Pr}, \tag{5}$$

with

$$\mathscr{L}_{mse} = \frac{1}{N_p} \sum_{i=1}^{N_p} (G_i(x, Pr) - y_i)^2, \tag{6}$$

$$\mathscr{L}_{Pr} = \frac{1}{N_p} \sum_{i=1}^{N_p} (G_i^P(x, G^U(x), Pr))^2, \tag{7}$$

where the first and second terms on the right-hand side in equation (5) are the cGAN loss and mean squared loss (MSE), respectively. The last term is the physical parameter loss, which

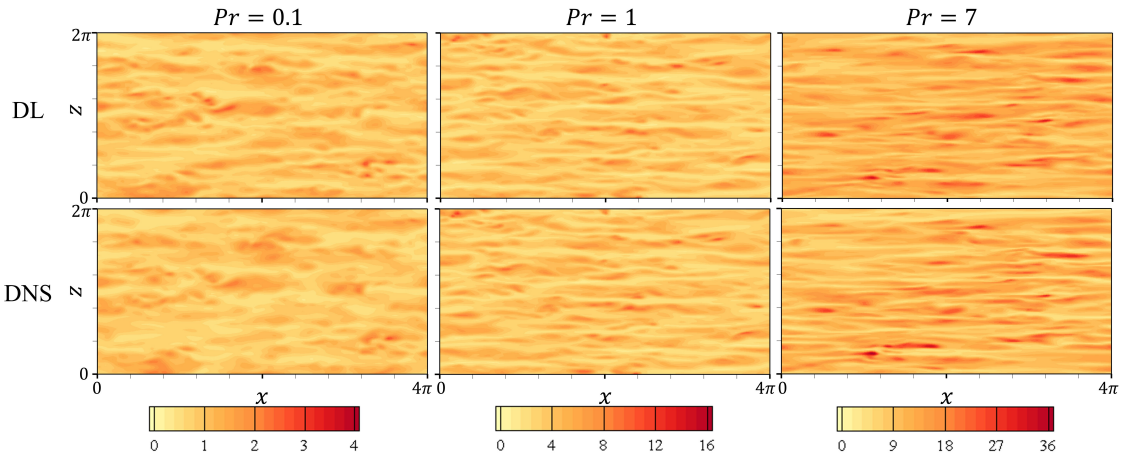

Figure 2. Instantaneous surface heat flux for Pr, which was not used in training, obtained from wall shear stresses using cGAN.

can decompose the surface heat flux into universal and Pr-dependent features. λ_1 and λ_2 are 10 and 200, respectively. In equation (6) and (7), N_p is the number of inputs, and $G(x)$ denotes the predicted surface heat flux through the generator. $G^P(x)$ and $G^U(x)$ are a Pr-dependent feature and the universal feature, respectively. In the training process, the parameters of the generator (G) are trained in the direction of minimizing $\mathscr{L}_{total}$, and the parameters of the discriminator (D) are trained in the direction of maximizing $\mathscr{L}_{cGAN}$.

RESULTS AND DISCUSSION

Prediction of surface heat flux with Pr

We apply cGAN with decomposition algorithm for prediction of surface heat flux with Pr from streamwise wall shear stress, spanwise wall shear stres and Prandtl number in turbulent channel flow. In figure 2, we qualitatively evaluated our model by considering for the surface heat flux with untrained Pr, which was not used in training. Our model generated surface heat flux field that was slightly overpredicted than one of DNS for the lowest $Pr = 0.1$, but the predicted field is similar to that of DNS. The surface heat flow for $Pr = 1$ and 7 predicted through cGAN well have the characteristics of the heat flow observed in DNS.

Table 1. Correlation coefficient between target data (DNS data) and surface heat flux with Pr predicted by the deep learning model.

		cGAN	CNN
trained Pr	0.2	0.890	0.909
	0.71	0.968	0.973
	2	0.975	0.979
	5	0.922	0.931
Untrained Pr	0.1	0.802	0.822
	0.4	0.918	0.937
	1	0.967	0.977
	3	0.945	0.958
	7	0.876	0.897

For qualitatively evaluation of the trained model, CNN was considered as a comparative model. First, we examined the correlation coefficient ($R = \left\langle q_w^{'DNS} q_w^{'DL} \right\rangle / (\sigma(q_w^{DNS})\sigma(q_w^{DL}))$; q_w is surface heat flux, and σ is standard deviation) between generated heat flux and that of DNS in table 1. Both cGAN and CNN were able to predict accurately at approximately 0.9 for all P except $Pr = 7$. Although the surface heat flux predicted through cGAN had a relatively slightly lower correlation coefficient compared to CNN, cGAN was able to generate a DNS-like surface heat flux. Additionally, probability density function(P.d.f.) of surface heat flux predicted through CNN and cGAN are presented in figure 3. For trained Pr in figure3*(a)*, CNN generated surface heat flux for all Pr that was slightly underestimated than that of DNS, but the heat flux predicted through cGAN was very similar to the distribution of DNS. Furthermore, we tested our model for surface heat flux for untrained Prandtl number in figure3*(b)*, which is not considered for learning. Similar to the results for the trained Prandtl number, the heat flux generated by CNN is underpredicted than the distribution of DNS. On the other hand, cGAN was able to predict similar to the results of DNS for strong heat flux. These results mean that our model can generate a heat flux that reflects the physical characteristics of the Prandtl number well. Although cGAN has slightly lower prediction accuracy than CNN in point-by-point statistics, we consider only cGAN with more accurate predictions for strong local heat fluxes, which are more important in turbulent heat transfer.

Interpretation of Pr-effect

For interpretation of the trained model, we analyzed the underlying physical properties between wall shear stresses and surface heat flux with respect to Pr through gradient maps obtained from the trained model. For reliable analysis, we focused on trained Pr, where our model made more accurate predictions in the previous section. The sensitivity analysis through gradient map can understand the relation between input and output, which has been applied to image classification and regression problems (Simonyan *et al.*, 2013; Kim & Lee, 2019). The gradient map is defined as follows.

$$S^k(i,j) = \frac{\partial N(I)}{\partial I^k(i,j)} \tag{8}$$

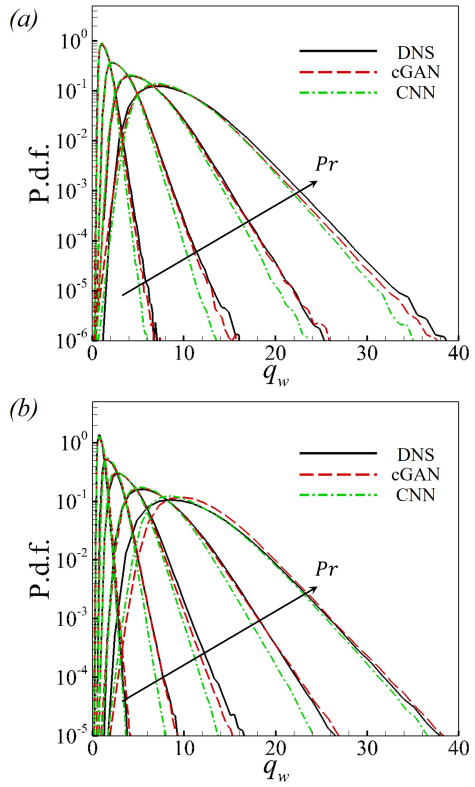

Figure 3. Probability density function (P.d.f.) of surface heat flux for *(a)* trained $Pr(=0.2, 0.71, 2, 5)$ and *(b)* untrained $Pr(=0.1, 0.4, 1, 3, 7)$ obtained through deep learning models.

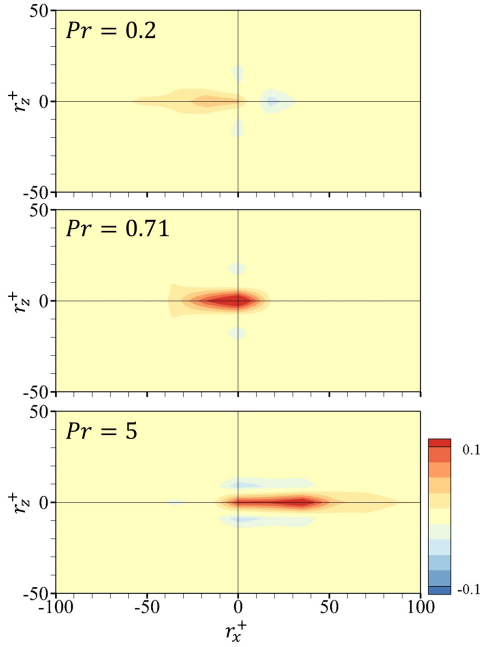

Figure 4. Average of gradient maps for streamwise wall shear stress with respect to surface heat flux for Pr obtained through cGAN.

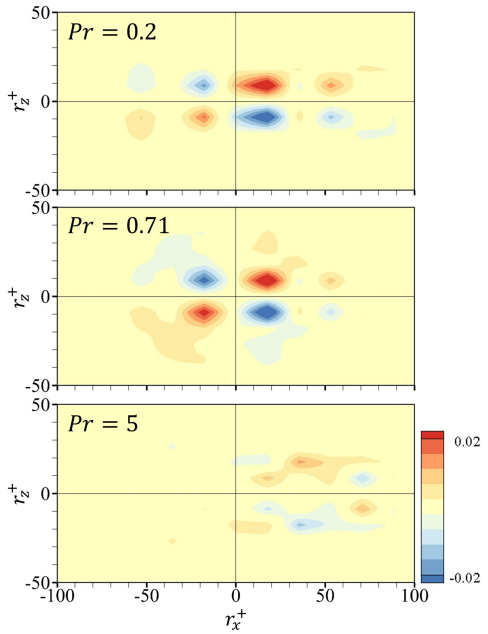

Figure 5. Average of gradient maps for spanwise wall shear stress with respect to surface heat flux for Pr obtained through cGAN.

where $S^k_{i,j}$ is gradient map for input $I^k(i,j)$ with respect to output $N(I)$. and i and j are indices in x- and z-direction. respectively. k is the input variable.

First, we investigate nonlinear relationship between streamwise wall shear stress and local heat flux, and the average gradients map between them for Pr are presented in figure 4. The positive peak moves from upstream to downstream with increasing Pr. It is relevant with that the temperature field is more dominated by large scale motion with decreasing Pr, which increases the convection velocity of temperature (Kowalewski *et al.*, 2003). For the average of gradient maps for spanwise wall shear stress in figure 5, the significant patterns are skew symmetricity($S^{\tilde{\tau}_{w,z}}_{i,j} = -S^{\tilde{\tau}_{w,z}}_{i,-j}$) for all Pr. The case of $Pr = 0.2, 0.71$ indicates that the local heat flux can be enhanced when the vortex pair is downstream or vortices cross diagonally at the center point, even though the streamwise wall shear stress is weak. The gradient for $Pr = 5$ is relatively weak, meaning that the surface heat flux at high Pr is weakly influenced by the spanwise wall shear stress compared with other Prandtl numbers. In short, we identified the nonlinear relationship between wall shear stresses and local heat flux for considering the Pr effect.

Next, for analysis of noticeable physical properties, we confirmed relationship between the decomposed features, universal and Pr-dependent features, and the surface heat flux obtained through the trained model. The two-point correlation between them are presented in figure 6. The universal feature had a high correlation coefficient with the surface heat flux for all Pr at $-50 < r_x^+ < 50$. This indicates that universal features reflect the common characteristics of surface heat flux regardless of Prandtl number. For relation between surface heat flux and Pr-dependent feature in figure6*(b)*, when $Pr > 1$, the high correlation coefficient between them is at $r_x^+ < 0$. On the other hand, a high correlation is observed at $r_x^+ > 0$ when $Pr < 1$. This result suggests that as the Prandtl number decreases, our model can extract features that well reflect the physical properties shown under the effect of large scale motion. These results imply that our model can automatically separate the surface heat flux with respect to Prandtl number without additional knowledge in the training process, and the decomposed features well reflect the influence on Prandtl number.

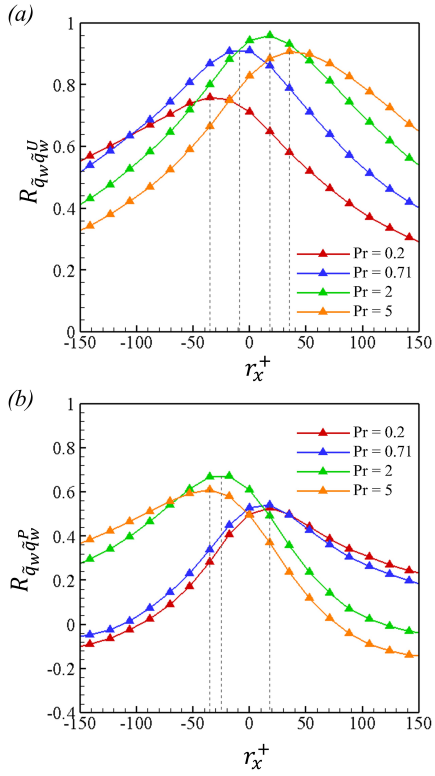

Figure 6. Two-point correlation along streamwise direction *(a)* between surface heat flux and universal features and *(b)* surface heat flux and Pr-dependent features.

CONCLUSION

We developed cGAN with a new decomposition algorithm to predict turbulent heat transfer with Pr. The model was able to generate well not only for the Prandtle numbers considered in the training process, but also for the thermal flux for the Prandtl numbers not used in the training. Our model quantitatively generated a more accurate surface heat flux for all Pr than that of comparative model, and the predicted heat flux very similar to the distribution of DNS.

For the interpretation of the trained model, we investigate gradient maps for wall shear stresses with respect to surface heat flux. Through the gradient map, we confirmed the nonlinear correlation between input and output well for Prandtl number, and our model well reflected the effect observed in the surface heat flux with Pr. Furthermore, our model can extract the effect of physical parameter based on turbulence data without detailed knowledge, allowing analysis of the physical parameter effect and the relationship between turbulence variables. Our framework would be extended to analyze effect of other physical parameters such as Reynolds number, discover physical phenomena in data, and understand deep learning of turbulent flows

Acknowledgments

This work was supported by National Research Foundation of Korea (NRF) grants funded by the Korean government (MSIP) (2017R1E1A1A03070282, 2022R1A2C2005538).

REFERENCES

Abe, H., Kawamura, H. & Matsuo, Y. 2004 Surface heat-flux fluctuations in a turbulent channel flow up to Re_τ=1020 with Pr=0.025 and 0.71. *Int. J. Heat Fluid Flow* **25** (3), 404–419.

Antonia, R.A., Krishnamoorthy, L.V. & Fulachier, L. 1988 Correlation between the longitudinal velocity fluctuation and temperature fluctuation in the near-wall region of a turbulent boundary layer. *Int. J. Heat Mass Transf.* **31** (4), 723–730.

Güemes, A., Discetti, S. & Ianiro, A. 2019 Sensing the turbulent large-scale motions with their wall signature. *Phys.Fluids* **31** (12), 125112.

Güemes, A., Discetti, S., Ianiro, A., Sirmacek, B., Azizpour, H. & Vinuesa, R. 2021 From coarse wall measurements to turbulent velocity fields through deep learning. *Phys. Fluids* **33** (7), 075121.

Jagodinski, E., Zhu, X. & Verma, S. 2020 Uncovering dynamically critical regions in near-wall turbulence using 3D convolutional neural networks. *arXiv preprint arXiv:2004.6187* .

Kasagi, N. & Ohtsubo, Y. 1993 Direct numerical simulation of low Prandtl number thermal field in a turbulent channel flow. In *Turbulent Shear Flows 8*, pp. 97–119. Springer.

Kasagi, N., Tomita, Y. & Kuroda, A. 1992 Direct numerical simulation of passive scalar field in a turbulent channel flow. *ASME J. Heat Transfer* **114** (3), 598–606.

Kawamura, H., Ohsaka, K., Abe, H. & Yamamoto, K. 1998 DNS of turbulent heat transfer in channel flow with low to medium-high prandtl number fluid. *Int. J. Heat Fluid Flow* **19** (5), 482–491.

Kim, H., Kim, J., Won, S. & Lee, C. 2021 Unsupervised deep learning for super-resolution reconstruction of turbulence. *J. Fluid Mech.* **910**, A29.

Kim, J. & Lee, C. 2019 Prediction of turbulent heat transfer using convolutional neural networks. *J. Fluid Mech.* **882**, A.

Kim, J. & Lee, C. 2020 Deep unsupervised learning of turbulence for inflow generation at various reynolds numbers. *J. Compu. Phys.* **406**, 109216.

Kim, J. & Moin, P. 1989 Transport of passive scalars in a turbulent channel flow. In *Turbulent Shear Flows 6*, pp. 85–96. Springer.

Kowalewski, T. A., Mosyak, A. & Hetsroni, G. 2003 Tracking of coherent thermal structures on a heated wall. *Exp. Fluids* **34** (3), 390–396.

Lu, Peter Y., Kim, Samuel & Soljačić, Marin 2020 Extracting interpretable physical parameters from spatiotemporal systems using unsupervised learning. *Phys. Rev. X* **10** (3), 031056.

Simonyan, K., Vedaldi, A. & Zisserman, A. 2013 Deep inside convolutional networks: Visualising image classification models and saliency maps. *arXiv preprint arXiv:1312.6034* .